JACS
JOURNAL OF THE AMERICAN CHEMICAL SOCIETY
Article
pubs.acs.org/JACS

Mechanisms and Origins of Switchable Chemoselectivity of Ni-Catalyzed C(aryl)−O and C(acyl)−O Activation of Aryl Esters with Phosphine Ligands

Xin Hong,[†] Yong Liang,[†] and K. N. Houk*

Department of Chemistry and Biochemistry, University of California, Los Angeles, California 90095, United States

Supporting Information

ABSTRACT: Many experiments have shown that nickel with monodentate phosphine ligands favors the C(aryl)−O activation over the C(acyl)−O activation for aryl esters. However, Itami and co-workers recently discovered that nickel with bidentate phosphine ligands can selectively activate the C(acyl)−O bond of aryl esters of aromatic carboxylic acids. The chemoselectivity with bidentate phosphine ligands can be switched back to C(aryl)−O activation when aryl pivalates are employed. To understand the mechanisms and origins of this switchable chemoselectivity, density functional theory (DFT) calculations have been conducted. For aryl esters, nickel with bidentate phosphine ligands cleaves C(acyl)−O and C(aryl)−O bonds via three-centered transition states. The C(acyl)−O activation is more favorable due to the lower bond dissociation energy (BDE) of C(acyl)−O bond, which translates into a lower transition-state distortion energy. However, when monodentate phosphine ligands are used, a vacant coordination site on nickel creates an extra Ni−O bond in the five-centered C(aryl)−O cleavage transition state. The additional interaction energy between the catalyst and substrate makes C(aryl)−O activation favorable. In the case of aryl pivalates, nickel with bidentate phosphine ligands still favors the C(acyl)−O activation over the C(aryl)−O activation at the cleavage step. However, the subsequent decarbonylation generates a very unstable *t*Bu-Ni(II) intermediate, and this unfavorable step greatly increases the overall barrier for generating the C(acyl)−O activation products. Instead, the subsequent C−H activation of azoles and C−C coupling in the C(aryl)−O activation pathway are much easier, leading to the observed C(aryl)−O activation products.

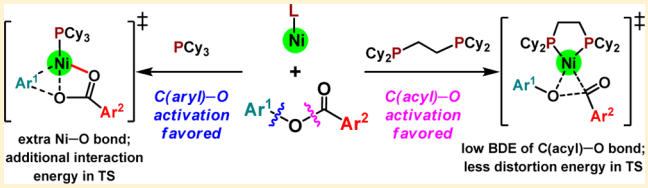

INTRODUCTION

Transition-metal-catalyzed cross-coupling reactions have become important tools for laboratorial and industrial carbon−carbon and carbon−heteroatom bond formations because of the efficiency and broad applicability of such reactions.[1] Despite the great success of cross-couplings using aryl halides and palladium catalysts,[2] extensive efforts toward environmentally friendly electrophiles and low-cost catalysts have led to the discovery of nickel-catalyzed C(aryl)−O activation.[3] In 2008, Garg and Shi independently reported the first nickel-catalyzed C(aryl)−O activation using aryl esters,[4] and other carbon electrophiles, such as carbamates,[5] sulfamates,[6] phosphates,[7] and even phenolates,[8] have seen increased use over the past few years. In addition, the design of nucleophiles for the C(aryl)−Ni intermediate has enabled not only C−C, but also C−N and C−H bond formations (Scheme 1).[5g,6c,7b,9]

Among the developed methodologies of Ni-catalyzed C−O activation of aryl esters using monodentate phosphine ligands, only the cleavage of C(aryl)−O bond occurs (Scheme 2a).[5f,9a,10] In addition, Itami and co-workers reported that nickel with a bidentate phosphine ligand, 1,2-bis-(dicyclohexylphosphino)ethane (dcype), can also favor the C(aryl)−O activation of aryl pivalates (Scheme 2b).[11] However, they later discovered that the same catalyst can achieve an unexpected C(acyl)-O activation and decarbonylation when aryl esters of aromatic carboxylic acids are employed (Scheme 2c).[12] On the basis of this strategy, a wide variety of heteroaromatic esters were smoothly coupled with azoles to generate bis(heteroaryl) scaffolds in a straightforward fashion.[13]

Scheme 1. Representative Reactions Involving Ni-Catalyzed C(aryl)−O Activation

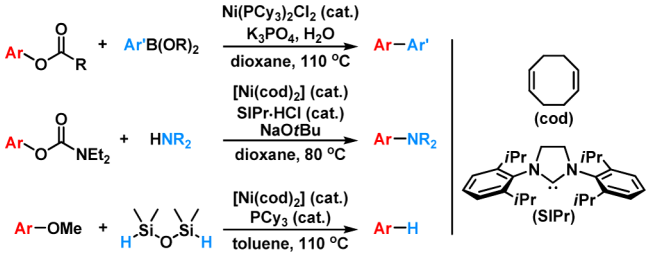

There are two possible catalytic cycles for the Ni/dcype catalyzed C−O activation of aryl esters (Scheme 3). For the pivalic ester, the C(aryl)−O activation occurs to give intermediate **A**. Subsequent azole C−H activation generates intermediate **B**, which undergoes the C_{sp2}−C_{sp2} reductive elimination to produce the observed cross-coupling product.

Received: November 20, 2013
Published: January 15, 2014

   dx.doi.org/10.1021/ja4118413 | J. Am. Chem. Soc. 2014, 136, 2017−2025

Scheme 2. Chemoselectivity of Ni-Catalyzed C−O Activation of Aryl Esters with Phosphine Ligands

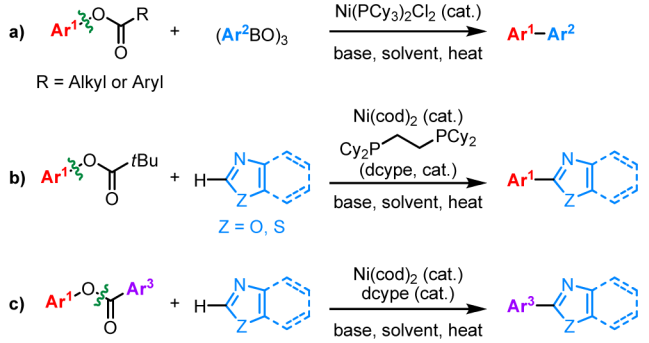

Scheme 3. Proposed Mechanisms for Ni-Catalyzed C−O Activation of Aryl Esters and Subsequent C−C Coupling with Azoles

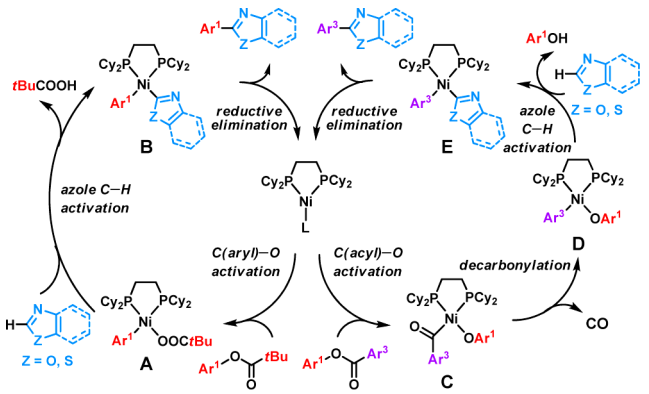

Alternatively, aromatic ester undergoes the C(acyl)−O activation to give intermediate **C**. Subsequent decarbonylation generates the aryl-nickel intermediate **D**. After the azole C−H activation, intermediate **E** undergoes reductive elimination to produce the cross-coupling product. Although the proposed mechanisms are plausible, the resting states, rate-determining steps, and especially the origins of chemoselectivity are not known. Therefore, we have used density functional theory (DFT) calculations to explore the mechanisms and origins of switchable chemoselectivity of Ni-catalyzed C(aryl)−O and C(acyl)−O activation of aryl esters with phosphine ligands.

COMPUTATIONAL METHODS

All density functional theory (DFT) calculations were performed with Gaussian 09.[14] Geometry optimization of all the minima and transition states involved was carried out at the B3LYP level of theory[15] with the SDD basis set[16] for nickel and the 6-31G(d) basis set[17] for the other atoms (keyword 5D was used in the calculations). The vibrational frequencies were computed at the same level to check whether each optimized structure is an energy minimum or a transition state and to evaluate its zero-point vibrational energy (ZPVE) and thermal corrections at 298 K. The single-point energies and solvent effects in 1,4-dioxane were computed at the M06 level of theory[18] with the SDD basis set for nickel and the 6-311+G(d,p) basis set for the other atoms, based on the gas-phase optimized structures. Solvation energies were evaluated by a self-consistent reaction field (SCRF) using the SMD model.[19] Fragment distortion and interaction energies and bond dissociation energies were computed at the M06/6-311+G(d,p)-SDD level using the B3LYP/6-31G(d)-SDD geometries in the gas phase. The initial geometry of PCy_3 was taken from the crystal structure of $Ni(PCy_3)(C_2H_4)_2$,[20] and the initial geometry of dcype was taken from the crystal structure of Ni(dcype)$(CO)_2$.[12] Several rotamers of the ligands in the nickel complexes were tested as the initial geometry in the optimizations, and extensive conformational searches for the benzoate and pivalate coordinated complexes have been conducted. The lowest energy conformers and isomers are shown in this work.

RESULTS AND DISCUSSION

Aryl Esters of Aromatic Carboxylic Acids: Origins of Ligand-Controlled Chemoselectivity of C−O Activation. Using phenyl benzoate and benzoxazole as model reactants, we first explored the mechanism of Ni/dcype catalyzed C−O activation of aromatic esters and subsequent C−C couplings with azoles. The free energy profile is shown in Figure 1, and optimized structures of selected intermediates and transition states are shown in Figure 2. From the substrate coordinated complex **1**, the C(acyl)−O activation via **TS2** requires an activation free energy of 19.1 kcal/mol to generate the C(acyl)−Ni intermediate **3**. For the C−O activation, three

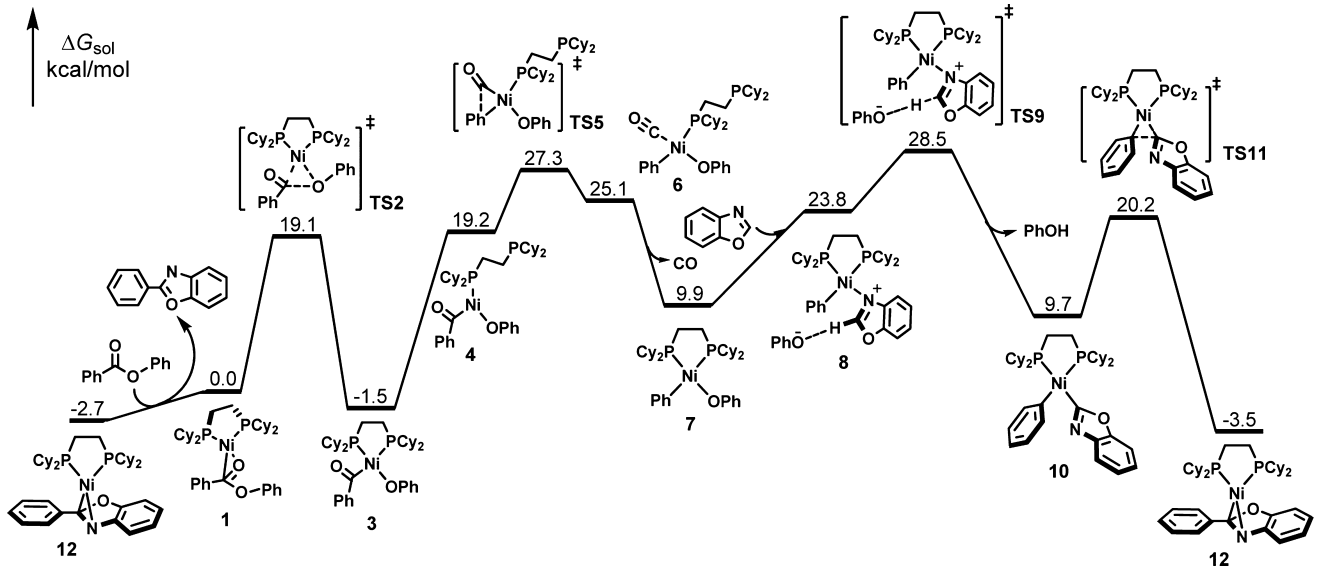

Figure 1. DFT-computed Gibbs free energies for the Ni/dcype-catalyzed decarbonylative C−C coupling of benzoxazole and phenyl benzoate.

dx.doi.org/10.1021/ja4118413 | J. Am. Chem. Soc. 2014, 136, 2017−2025

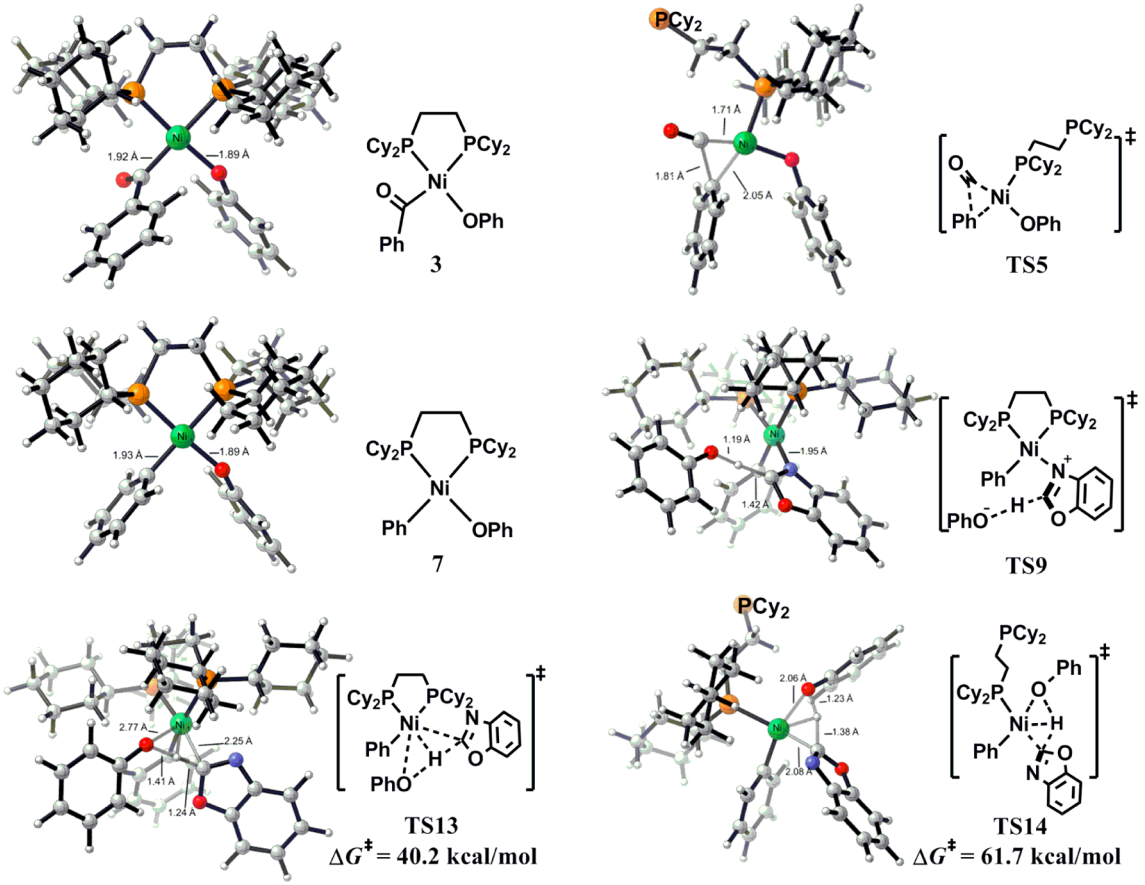

Figure 2. DFT-optimized structures of selected intermediates and transition states for the Ni/dcype-catalyzed decarbonylative C−C coupling of benzoxazole and phenyl benzoate.

possible pathways were explored, and the origins of preferences are discussed in detail later. After the C(acyl)−O activation, a change from κ^2 to κ^1 coordination of the dcype ligand is necessary to provide a coordination site for the carbonyl migration through transition state **TS5**. The dissociation of one of the diphosphine arms is endergonic by 20.7 kcal/mol, and this contributes to the high overall barrier (28.8 kcal/mol) for carbonyl migration. After carbonyl migration, a barrierless decarbonylation occurs to produce the tetra-coordinated nickel complex **7**. From **7**, the substitution of phenoxide by benzoxazole gives the N-coordinated nickel intermediate **8**. This step is endergonic by 13.9 kcal/mol. The following deprotonation of benzoxazole using phenoxide as base via **TS9** is facile, requiring an activation free energy of only 4.7 kcal/mol. Besides **TS9**, two additional transition states of four-centered σ-bond metathesis, **TS13** and **TS14**, are also located (Figure 2). Comparing **TS13** with **TS14**, **TS13** is significantly more stable because it maintains the bidentate coordination of the dcype ligand. However, the σ-bond metathesis pathway via **TS13** is disfavored by 11.7 kcal/mol in terms of free energy than the stepwise deprotonation pathway via **TS9** (40.2 versus 28.5 kcal/mol). The similar preference was also reported in previous studies of Pd-catalyzed C−H activation of oxazoles and thiazoles.[21] After the C−H activation, intermediate **10** undergoes a C_{sp2}−C_{sp2} reductive elimination to give the product coordinated complex **12**. Subsequent product extrusion from **12** to regenerate substrate coordinated complex **1** is endergonic by 2.7 kcal/mol, suggesting that **12** is the resting state of the catalytic cycle. Therefore, the overall barrier for this reaction is 31.2 kcal/mol, which is close to the value expected under the experimental conditions (150 °C and 24 h in 1,4-dioxane).[12]

Besides the C(acyl)−O activation of aryl esters of aromatic carboxylic acids, the competing C(aryl)−O activation was also explored. The free energy profile is shown in Figure 3. There are two possible C(aryl)−O activation pathways with dcype

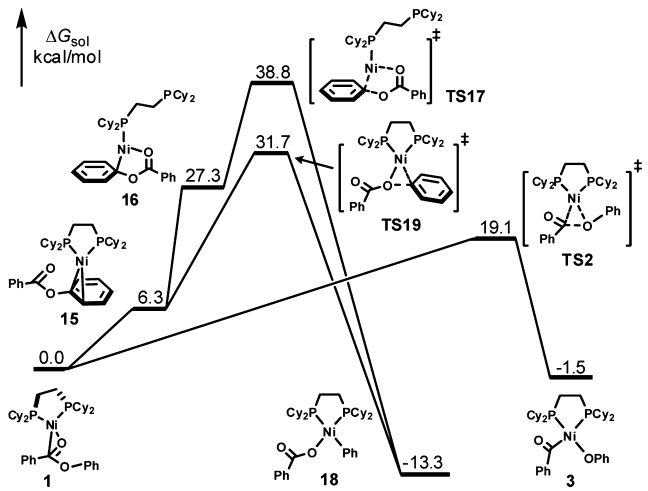

Figure 3. DFT-computed Gibbs free energies for the Ni/dcype-catalyzed C(acyl)−O and C(aryl)−O activation pathways of phenyl benzoate.

dx.doi.org/10.1021/ja4118413 | J. Am. Chem. Soc. 2014, 136, 2017−2025

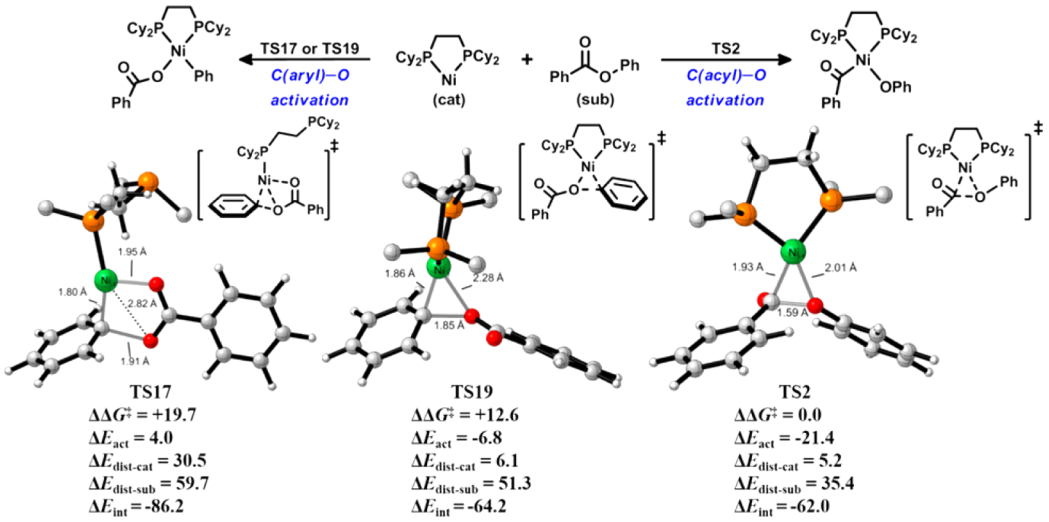

Figure 4. The distortion/interaction analysis of the C(aryl)–O and C(acyl)–O activation transition states involving the Ni/dcype catalyst (only the α-carbon of cyclohexyl group is shown for simplicity; energies are in kcal/mol).

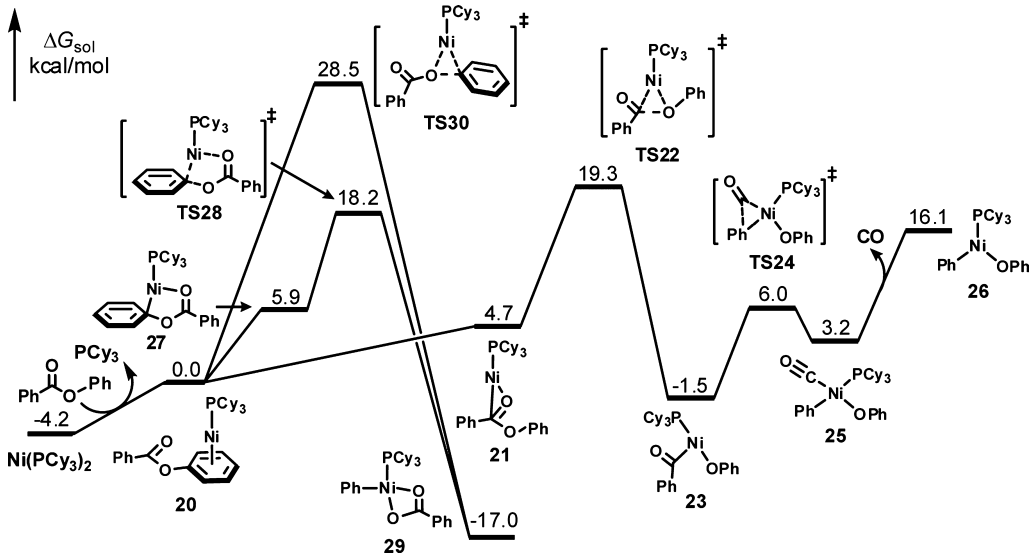

Figure 5. DFT-computed Gibbs free energies for the Ni/PCy_3-catalyzed C(acyl)–O and C(aryl)–O activation pathways of phenyl benzoate.

acting as either a mono- or bidentate ligand. When dcype acts as a bidentate ligand, nickel migrates to the oxygenated phenyl group in **15** in order to undergo the C(aryl)–O bond cleavage via **TS19**. The migration is endergonic by 6.3 kcal/mol, and the C(aryl)–O bond cleavage requires an activation free energy of 25.4 kcal/mol, resulting in an overall barrier of 31.7 kcal/mol. The generated phenylnickel(II) benzoate **18** is 13.3 kcal/mol more stable than the Ni–substrate complex **1**. If dcype acts as a monodentate ligand, then the coordination of acyl oxygen leads to the five-centered transition state **TS17**. Although the barrier for the cleavage step from intermediate **16** is only 11.5 kcal/mol, the formation of **16** is very endergonic, making the overall barrier as high as 38.8 kcal/mol. Therefore, compared with the C(aryl)–O activation via **TS17** or **TS19**, the Ni/dcype catalyst significantly favors the C(acyl)–O activation via the three-centered transition state **TS2** (19.1 kcal/mol, Figure 3).

To gain insights into the origins of chemoselectivity of Ni/dcype-catalyzed C–O activation of aryl esters, we analyzed the C(acyl)–O and C(aryl)–O activation transition states using the distortion/interaction model,[22−24] as shown in Figure 4. Each transition structure was separated into two fragments (the distorted catalyst and substrate), followed by single point energy calculations on each distorted fragment. The energy differences between the distorted structures and optimized ground-state structures are the distortion energy of Ni(dcype) catalyst ($\Delta E_{\text{dist-cat}}$) and aryl ester substrate ($\Delta E_{\text{dist-sub}}$), respectively. The interaction energy (ΔE_{int}) is the difference between the activation energy (ΔE_{act}) and the total distortion energy ($\Delta E_{\text{dist-cat}} + \Delta E_{\text{dist-sub}}$).

For the C(aryl)–O activation transition states, **TS17** and **TS19**, the distortion energy of the Ni(dcype) catalyst, $\Delta E_{\text{dist-cat}}$, causes **TS19** to be lower in energy. Although the interaction energy, ΔE_{int}, is larger in **TS17** because of the extra Ni–O(acyl) bond, dissociating one of the diphosphine arms from nickel results in a very high distortion energy of catalyst (30.5 kcal/mol, Figure 4), making the five-centered transition state **TS17** unfavorable for the C(aryl)–O activation. Comparing the three-centered C(acyl)–O and C(aryl)–O activation transition states, **TS2** and **TS19**, they have similar $\Delta E_{\text{dist-cat}}$ and ΔE_{int}, but very different distortion energy of substrate, $\Delta E_{\text{dist-sub}}$. The

dx.doi.org/10.1021/ja4118413 | J. Am. Chem. Soc. 2014, 136, 2017−2025

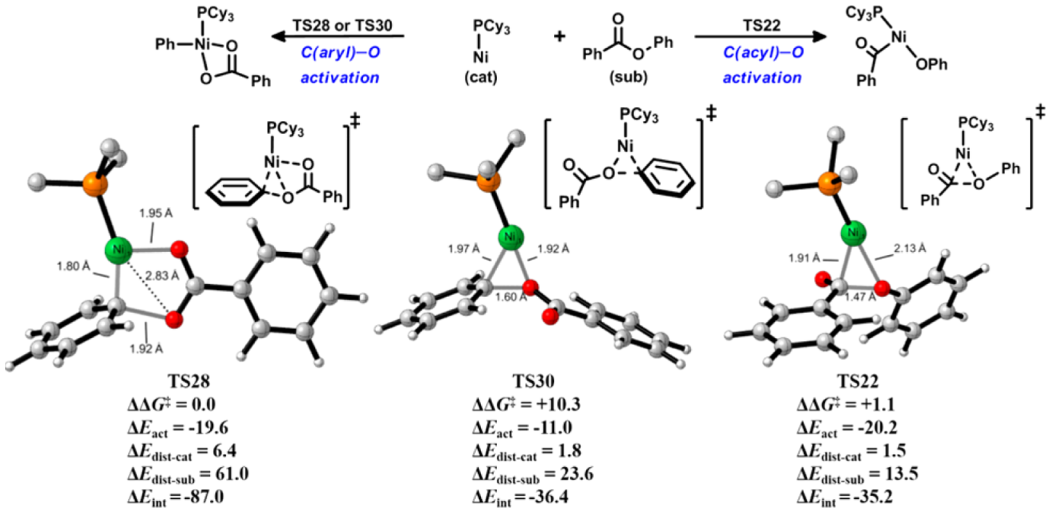

Figure 6. The distortion/interaction analysis of the C(aryl)–O and C(acyl)–O activation transition states involving the Ni/PCy_3 catalyst (only the α-carbon of cyclohexyl group is shown for simplicity; energies are in kcal/mol).

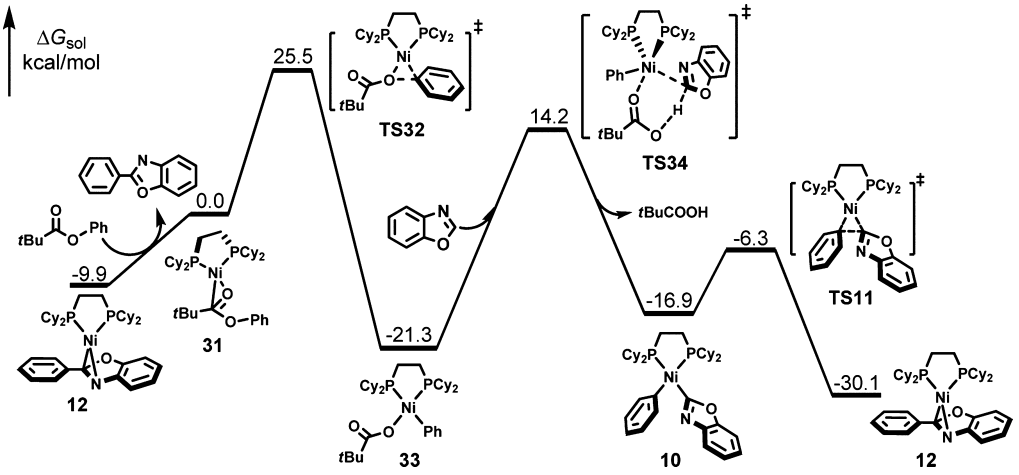

Figure 7. DFT-computed Gibbs free energies for the Ni/dcype-catalyzed C–C coupling between benzoxazole and phenyl pivalate.

lower $\Delta E_{dist\text{-}sub}$ of **TS2** (35.4 versus 51.3 kcal/mol, Figure 4) leads to the preference for the C(acyl)–O activation. The computed homolytic dissociation energy of C(aryl)–O bond of phenyl benzoate is 101.3 kcal/mol, and the value of the C(acyl)–O bond is 78.2 kcal/mol. This indicates that the C(acyl)–O bond is much weaker than the C(aryl)–O bond. The weaker C(acyl)–O bond requires less distortion of the substrate in the three-centered C–O cleavage transition state. Therefore, the C(acyl)–O activation is favorable using nickel catalysts with bidentate phosphine ligands.

We also investigated the possible C–O activation pathways with the Ni/PCy_3 catalyst. As shown in Figure 5, the formation of active Ni(PCy_3)–substrate complex **20** from Ni(PCy_3)$_2$ is endergonic by 4.2 kcal/mol.[25] The C(acyl)–O cleavage from **20** via **TS22** requires an activation free energy of 19.3 kcal/mol. The subsequent decarbonylation gives a relatively unstable intermediate **26** for transmetalation. For the C(aryl)–O activation from **20** to intermediate **29**, the three-centered transition state **TS30** is much less stable than the five-centered transition state **TS28**. The barrier for the C(aryl)–O activation pathway via **TS28** is 18.2 kcal/mol, which is 1.1 kcal/mol lower than that of the C(acyl)–O activation with the monodentate PCy_3 ligand (**TS22:** 19.3 kcal/mol, Figure 5).[26] In addition to the preference for the C(aryl)–O activation transition state, the different stabilities of the generated intermediates, **26** (16.1 kcal/mol) and **29** (−17.0 kcal/mol), could lead to even larger preference for the C(aryl)–O activation pathway when the subsequent transformations are not facile. A previous computational study by Liu and co-workers showed that the transmetalation of boron reagents could have an barrier of over 30 kcal/mol.[10] In this case, the preference to the C(aryl)–O activation mainly arises from the much better stability of intermediate **29**.

The distortion/interaction analysis revealed the origins of the reversed chemoselectivity with the monodentate phosphine ligand (Figure 6). Comparing the three-centered transition states **TS30** and **TS22**, the weaker C(acyl)–O bond leads to the lower $\Delta E_{dist\text{-}sub}$ in **TS22** (13.5 versus 23.6 kcal/mol, Figure 6) and a 9.2 kcal/mol preference to break this bond. However, in the case of five-centered C(aryl)–O cleavage transition state **TS28**, the Ni(PCy_3) catalyst does not require as much distortion energy as the Ni(dcype) catalyst in **TS17** (30.5 kcal/mol, Figure 4), and thus the larger ΔE_{int} from the additional Ni–O bond (−87.0 kcal/mol, Figure 6) overrides the distortion penalty and leads to the overall preference to the C(aryl)–O bond activation with the Ni/PCy_3 catalyst.

dx.doi.org/10.1021/ja4118413 | J. Am. Chem. Soc. 2014, 136, 2017–2025

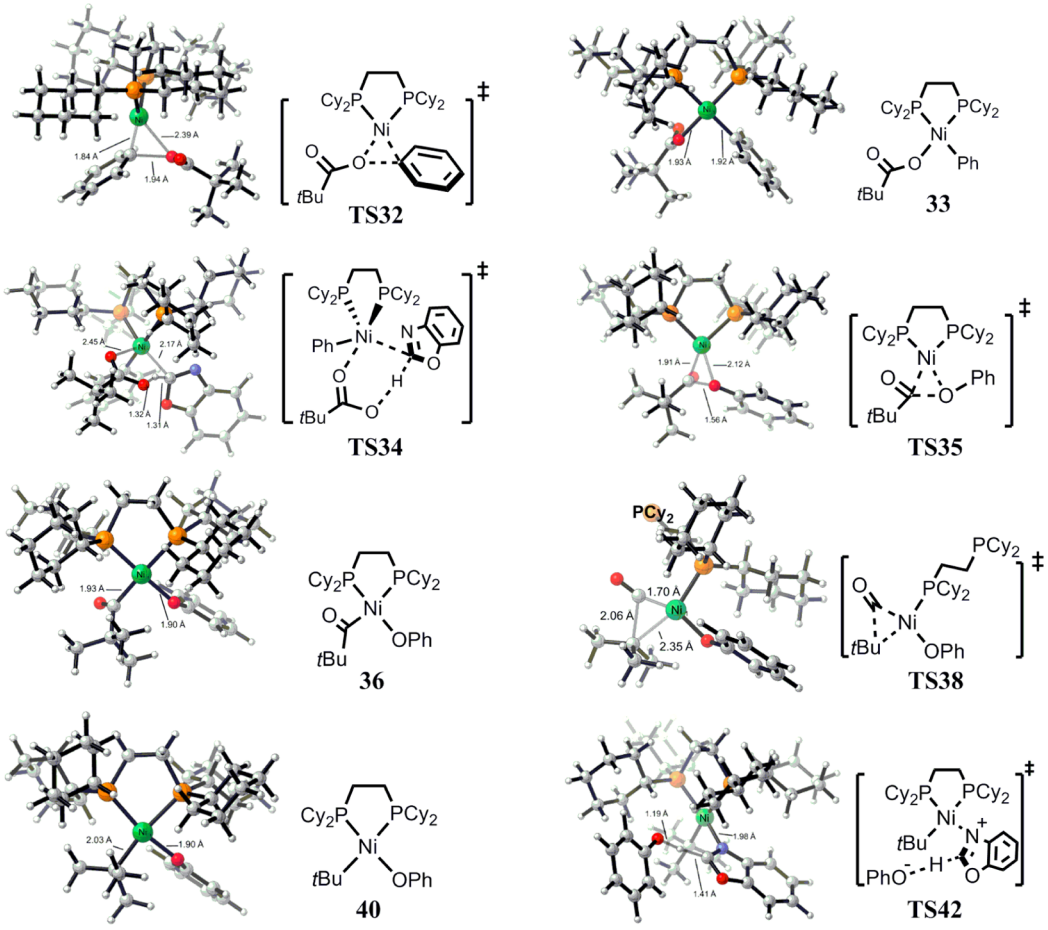

Figure 8. DFT-optimized structures of selected intermediates and transition states for the C(acyl)−O and C(aryl)−O activation pathways of the Ni/dcype-catalyzed C−C coupling between benzoxazole and phenyl pivalate.

Aryl Pivalates: Origins of Substrate-Dependent Chemoselectivity of C−O Activation. Unlike the Ni/dcype catalyzed C(acyl)−O activation of aryl esters of aromatic carboxylic acids, the C(aryl)−O activation of aryl pivalates was observed with the same catalyst (Scheme 2c). Using phenyl pivalate and benzoxazole as the model reactants, we studied the mechanism and origins of chemoselectivity of the Ni/dcype-catalyzed C−C couplings between azoles and aryl pivalates. The free energy profile is shown in Figure 7, and optimized structures of selected intermediates and transition states are shown in Figure 8. From the substrate coordinated complex **31**, the C(aryl)−O activation via **TS32** requires an activation free energy of 25.5 kcal/mol. This step is exergonic by 21.3 kcal/mol, suggesting that the resulting intermediate **33** is very stable. Then intermediate **33** undergoes a six-centered concerted metalation-deprotonation (CMD) pathway through transition state **TS34** to realize the benzoxazole C−H activation.[27] The subsequent C_{sp2}−C_{sp2} reductive elimination is facile with a barrier of 10.6 kcal/mol, giving the product coordinated complex **12**. The product extrusion from **12** is endergonic by 9.9 kcal/mol. For the whole catalytic cycle, both the C(aryl)−O activation and the benzoxazole C−H activation have high barriers, and the overall free energy span is 35.5 kcal/mol.

Very recently, Itami and co-workers reported an experimental mechanistic study of the same reaction.[28] They found that the stoichiometric reaction of naphthalen-2-yl pivalate with $Ni(cod)_2$/dcype gives an arylnickel(II) pivalate complex **33-n** (Scheme 4), which is proved an isolatable intermediate in the

Scheme 4. DFT-Computed Gibbs Free Energies for Reaction Using Naphthalen-2-yl Pivalate

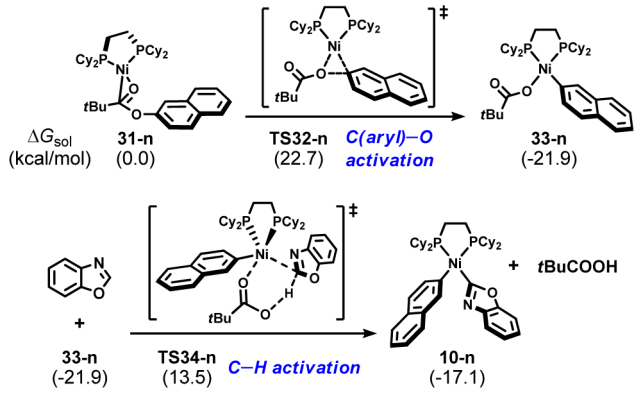

catalytic cycle. This is in good agreement with our computational results (Figure 7). Furthermore, kinetic studies reveal that the C−H activation of benzoxazole is the rate-determining step in the reaction using naphthalen-2-yl pivalate.[28] For a direct comparison, we also studied the C(aryl)−O activation pathway of naphthalen-2-yl pivalate (Scheme 4). It was found that naphthalen-2-yl pivalate is more reactive toward oxidative addition. The C(aryl)−O activation barrier is now 22.7 kcal/mol, which is 2.8 kcal/mol lower than the corresponding value for phenyl pivalate (25.5 kcal/mol, Figure 7). However, the C−H activation barrier is not affected by switching the phenyl

dx.doi.org/10.1021/ja4118413 | J. Am. Chem. Soc. 2014, 136, 2017−2025

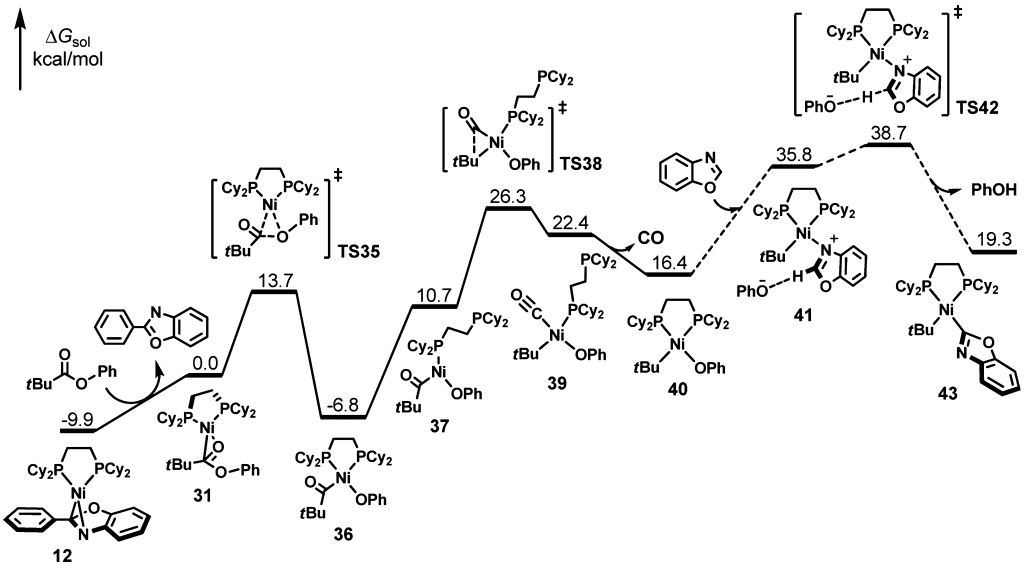

Figure 9. DFT-computed Gibbs free energies for the Ni/dcype-catalyzed decarbonylative C−C coupling of benzoxazole and phenyl pivalate.

Scheme 5. Comparisons of Reaction Free Energies of Decarbonylation Involving Benzoate and Pivalate

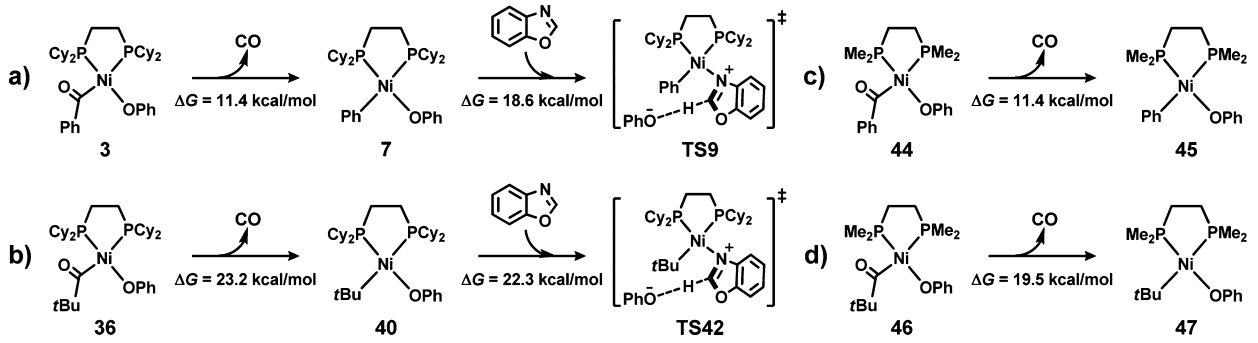

group (35.5 kcal/mol, Figure 7) to the naphthalen-2-yl group (35.4 kcal/mol, Scheme 4). Therefore, the rate-determining step of the reaction using naphthalen-2-yl pivalate is the C−H activation of benzoxazole.

The possible C(acyl)−O activation and subsequent decarbonylative C−C coupling were also studied. The free energy profile is shown in Figure 9, and optimized structures of selected intermediates and transition states are shown in Figure 8. From the substrate coordinated complex **31**, the C(acyl)−O activation via **TS35** is very facile, requiring an activation free energy of 13.7 kcal/mol. The generated intermediate **36** is exergonic by only 6.8 kcal/mol, suggesting that the C(acyl)−O activation step is reversible. The change from κ^2 to κ^1 coordination of the dcype ligand to nickel provides an open site for carbonyl migration via **TS38**. Subsequent decarbonylation generates an unstable intermediate **40**. From **40**, the further transformation with benzoxazole would lead to a very high-energy transition state **TS42** (38.7 kcal/mol, Figure 9). Comparing the two C−O activation transition states of phenyl pivalate, **TS32** (25.5 kcal/mol, Figure 7) and **TS35** (13.7 kcal/mol, Figure 9), the preference for the C(acyl)−O activation with bidentate phosphine ligands (Figure 4) still exists. However, the following C−H activation process requires an overall activation free energy of 45.5 kcal/mol (from **36** to **TS42**, Figure 9), which is 10.0 kcal/mol higher than that of the C−H activation after the C(aryl)−O bond cleavage shown in Figure 7. Therefore, when aryl pivalates are employed, the decarbonylative C−C coupling products are not observed.[11]

We further studied the origins of different barriers for the C−H activation processes after the C(acyl)−O bond cleavage of aromatic and pivalic esters. In the case of phenyl benzoate, the overall barrier is 30.0 kcal/mol and includes two parts shown in Scheme 5a: the reaction free energy of decarbonylation from intermediate **3** to **7** (11.4 kcal/mol)[29] and the barrier for the deprotonation of benzoxazole from intermediate **7** to transition state **TS9** (18.6 kcal/mol). Similarly, the 45.5 kcal/mol barrier in the case of phenyl pivalate also includes these two parts (Scheme 5b), and the major difference comes from the reaction free energy of decarbonylation. For phenyl pivalate, this step is endergonic by 23.2 kcal/mol, significantly higher than that for phenyl benzoate (11.4 kcal/mol, Scheme 5a). When using a less steric demanding ligand, 1,2-bis(dimethylphosphino)-ethane (dmpe), the decarbonylation is still endergonic by 11.4 kcal/mol for phenyl benzoate (Scheme 5c), while the reaction free energy for phenyl pivalate is 19.5 kcal/mol (Scheme 5d), 3.7 kcal/mol lower as compared to using the dcype ligand. This suggests that the steric repulsion between the bulky phosphine ligand and the *t*Bu group in intermediate **40** contributes to part of the difference between benzoate and pivalate. The electronic effect is the major reason for the extremely unfavorable decarbonylation in the case of pivalic esters. For both benzoate and pivalate, there are strong d_{Ni}-π^*_{acyl} interactions[30] in the C(acyl)−O activation products **3**, **36**,

dx.doi.org/10.1021/ja4118413 | J. Am. Chem. Soc. 2014, 136, 2017−2025

44, and **46**. After the decarbonylation, the phenyl group in intermediates **7** and **45** is a weak π acceptor, and the d_{Ni}-π^* interaction decreases, making this step endergonic by 11.4 kcal/mol (Scheme 5a,c). However, the *t*Bu group in intermediates **40** and **47** are unlikely to accept the d electrons from nickel, and the lack of the d-π^* interaction leads to much more endergonic decarbonylations (Scheme 5b,d).

CONCLUSIONS

Mechanisms and origins of the switchable chemoselectivity of the Ni-catalyzed C(acyl)−O and C(aryl)−O activation of aryl esters with phosphine ligands are revealed through DFT calculations. For aryl esters of aromatic carboxylic acids, the nickel with the bidentate dcype ligand cleaves the C−O bonds via three-centered transition states. The lower BDE of the C(acyl)−O bond leads to the lower distortion energy in the cleavage transition state, making the C(acyl)−O activation more favorable. After the facile C(acyl)−O activation, the endergonic dissociation of one of the diphosphine arms from nickel provides a coordination site for decarbonylation. Subsequently, the deprotonation of azoles by aryloxide realizes the C−H activation process. The following C_{sp2}−C_{sp2} reductive elimination generates the cross-coupling product. When the monodentate PCy_3 ligand is used with aryl esters, a vacant coordination site on nickel creates an extra Ni−O bond in the five-centered C(aryl)−O cleavage transition state. This additional interaction energy overrides the distortion penalty and makes the C(aryl)−O activation preferred.

For aryl pivalates, the nickel with bidentate phosphine ligand still favors the C(acyl)−O cleavage. However, the subsequent decarbonylation generates a highly unstable *t*Bu-Ni(II) intermediate due to the lack of d-π^* interaction between nickel and the *t*Bu group as well as the steric repulsion between the bulky phosphine ligand and the *t*Bu group. This very unfavorable step significantly increases the overall barrier for generating the C(acyl)−O activation products. Instead, the C−H activation of azoles and C−C coupling after the C(aryl)−O activation are much easier, leading to the observed C(aryl)−O activation products.

ASSOCIATED CONTENT

Supporting Information

Coordinates and energies of DFT-computed stationary points. This material is available free of charge via the Internet at http://pubs.acs.org.

AUTHOR INFORMATION

Corresponding Author

houk@chem.ucla.edu

Author Contributions

†These authors contributed equally.

Notes

The authors declare no competing financial interest.

ACKNOWLEDGMENTS

We thank Prof. Neil K. Garg and Dr. Peng Liu at UCLA for helpful discussions. We are grateful to the National Science Foundation (CHE-1059084) for financial support of this research. Calculations were performed on the Hoffman2 cluster at UCLA and the Extreme Science and Engineering Discovery Environment (XSEDE), which is supported by the NSF (OCI-1053575).

REFERENCES

(1) (a) Miyaura, N., Ed. *Topics in Current Chemistry*, Vol. *219*; Springer-Verlag: New York, 2002. (b) Hassan, J.; Sévignon, M.; Gozzi, C.; Schulz, E.; Lemaire, M. *Chem. Rev.* **2002**, *102*, 1359. (c) Diederich, F., Meijere, A., Eds. *Metal-Catalyzed Cross-Coupling Reactions*; Wiley-VCH: Weinheim, 2004. (d) Corbet, J.; Mignani, G. *Chem. Rev.* **2006**, *106*, 2651. (e) Negishi, E. *Bull. Chem. Soc. Jpn.* **2007**, *80*, 233. (f) Molander, G. A.; Ellis, N. *Acc. Chem. Res.* **2007**, *40*, 275. (g) Alberico, D.; Scott, M. E.; Lautens, M. *Chem. Rev.* **2007**, *107*, 174. (h) Ackermann, L.; Vicente, R.; Kapdi, A. R. *Angew. Chem., Int. Ed.* **2009**, *48*, 9792. (i) Chen, X.; Engle, K. M.; Wang, D.-H.; Yu, J.-Q. *Angew. Chem., Int. Ed.* **2009**, *48*, 5094. (j) Yamaguchi, J.; Yamaguchi, A. D.; Itami, K. *Angew. Chem., Int. Ed.* **2012**, *51*, 8960.

(2) (a) Old, D. W.; Wolfe, J. P.; Buchwald, S. L. *J. Am. Chem. Soc.* **1998**, *120*, 9720. (b) Littke, A. F.; Fu, G. C. *Angew. Chem., Int. Ed.* **2002**, *41*, 4176. (c) Nicolaou, K. C.; Bulger, P. G.; Sarlah, D. *Angew. Chem., Int. Ed.* **2005**, *44*, 4442. (d) Chinchilla, R.; Nájera, C. *Chem. Rev.* **2007**, *107*, 874. (e) Yin, L.; Liebscher, J. *Chem. Rev.* **2007**, *107*, 133. (f) Ming, C.; Kwong, F. Y. *Chem. Soc. Rev.* **2011**, *40*, 4963. (g) Li, B.-J.; Yu, D.-G.; Sun, C.-L.; Shi, Z.-J. *Chem.—Eur. J.* **2011**, *17*, 1728. (h) Seechurn, C. C. C. J.; Kitching, M. W.; Colacot, T. J.; Snieckus, V. *Angew. Chem., Int. Ed.* **2012**, *51*, 5062.

(3) For reviews, see (a) Yu, D.-G.; Li, B.-J.; Shi, Z.-J. *Acc. Chem. Res.* **2010**, *43*, 1486. (b) Rosen, B. M.; Quasdorf, K. W.; Wilson, D. A.; Zhang, N.; Resmerita, A.-M.; Garg, N. K.; Percec, V. *Chem. Rev.* **2011**, *111*, 1346. (c) Han, F. -S. *Chem. Soc. Rev.* **2013**, *42*, 5270. (d) Yamaguchi, J.; Muto, K.; Itami, K. *Eur. J. Org. Chem.* **2013**, 19. (e) Mesganaw, T.; Garg, N. K. *Org. Process Res. Dev.* **2013**, *17*, 29. For related studies on mechanism, see: (f) Yoshikai, N.; Matsuda, H.; Nakamura, E. *J. Am. Chem. Soc.* **2008**, *130*, 15258. (g) Yoshikai, N.; Matsuda, H.; Nakamura, E. *J. Am. Chem. Soc.* **2009**, *131*, 9590. (h) Xue, L.-Q.; Lin, Z.-Y. *Chem. Soc. Rev.* **2010**, *39*, 1692. (i) Li, Z.; Jiang, Y.-Y.; Fu, Y. *Chem.—Eur. J.* **2012**, *18*, 4345. (j) Yu, H.-Z.; Fu, Y. *Chem.—Eur. J.* **2012**, *18*, 16765. (k) Cornella, J.; Gómez-Bengoa, E.; Martin, R. *J. Am. Chem. Soc.* **2013**, *135*, 1997.

(4) (a) Quasdorf, K. W.; Tian, X.; Garg, N. K. *J. Am. Chem. Soc.* **2008**, *130*, 14422. (b) Guan, B.-T.; Wang, Y.; Li, B.-J.; Yu, D.-G.; Shi, Z.-J. *J. Am. Chem. Soc.* **2008**, *130*, 14468. (c) Li, B.-J.; Li, Y.-Z.; Lu, X.-Y.; Liu, J.; Guan, B.-T.; Shi, Z.-J. *Angew. Chem., Int. Ed.* **2008**, *47*, 10124. (d) Shimasaki, T.; Tobisu, M.; Chatani, N. *Angew. Chem., Int. Ed.* **2010**, *49*, 2929. (e) Ehle, A. R.; Zhou, Q.; Watson, M. P. *Org. Lett.* **2012**, *14*, 1202.

(5) (a) Sengupta, S.; Leite, M.; Raslan, D. S.; Quesnelle, C.; Snieckus, V. *J. Org. Chem.* **1992**, *57*, 4066. (b) Dallaire, C.; Kolber, I.; Gingras, M. *Org. Synth.* **2002**, *78*, 42. (c) Quasdorf, K. W.; Riener, M.; Petrova, K. V.; Garg, N. K. *J. Am. Chem. Soc.* **2009**, *131*, 17748. (d) Antoft-Finch, A.; Blackburn, T.; Snieckus, V. *J. Am. Chem. Soc.* **2009**, *131*, 17750. (e) Xi, L.; Li, B.-J.; Wu, Z.-H.; Lu, X.-Y.; Guan, B.-T.; Wang, B.-Q.; Zhao, K.-Q.; Shi, Z.-J. *Org. Lett.* **2010**, *12*, 884. (f) Quasdorf, K. W.; Antoft-Finch, A.; Liu, P.; Silberstein, A. L.; Komaromi, A.; Blackburn, T.; Ramgren, S. D.; Houk, K. N.; Snieckus, V.; Garg, N. K. *J. Am. Chem. Soc.* **2011**, *133*, 6352. (g) Hie, L.; Ramgren, S. D.; Mesganaw, T.; Garg, N. K. *Org. Lett.* **2012**, *14*, 4182. (h) Ramgren, S. D.; Hie, L.; Ye, Y.-X.; Garg, N. K. *Org. Lett.* **2013**, *15*, 3950.

(6) (a) Macklin, T. K.; Snieckus, V. *Org. Lett.* **2005**, *7*, 2519. (b) Wehn, P. M.; Du Bois, J. *Org. Lett.* **2005**, *7*, 4685. (c) Ramgren, S. D.; Silberstein, A. L.; Yang, Y.; Garg, N. K. *Angew. Chem., Int. Ed.* **2011**, *50*, 2171. (d) Chen, G.-J.; Han, F.-S. *Eur. J. Org. Chem.* **2012**, 3575.

(7) (a) Chen, H.; Huang, Z.-B.; Hu, X.-M.; Tang, G.; Xu, P.-X.; Zhao, Y.-F.; Cheng, C.-H. *J. Org. Chem.* **2011**, *76*, 2338. (b) Huang, J.-H.; Yang, L. M. *Org. Lett.* **2011**, *13*, 3750.

(8) (a) Yu, D.-G.; Li, B.-J.; Zheng, S.-F.; Guan, B.-T.; Wang, B.-Q.; Shi, Z.-J. *Angew. Chem., Int. Ed.* **2010**, *49*, 4566. (b) Yu, D.-G.; Shi, Z.-J. *Angew. Chem., Int. Ed.* **2011**, *50*, 7097.

(9) For C−N bond formations, see: (a) Mesganaw, T.; Silberstein, A. L.; Ramgren, S. D.; Nathel, N. F. F.; Hong, X.; Liu, P.; Garg, N. K. *Chem. Sci.* **2011**, *2*, 1766. (b) Llies, L.; Matsubara, T.; Nakamura, E. *Org. Lett.* **2012**, *14*, 5570. For C−H bond formations, see: (c) Álvarez-Bercedo, P.; Martin, R. *J. Am. Chem. Soc.* **2010**, *132*,

17352. (d) Tobisu, M.; Chatani, N. *ChemCatChem* **2011**, *3*, 1410. (e) Tobisu, M.; Yamakawa, K.; Shimasaki, T.; Chatani, N. *Chem. Commun.* **2011**, *47*, 2946. (f) Mesganaw, T.; Nathel, N. F. F.; Garg, N. K. *Org. Lett.* **2012**, *14*, 2918.
(10) Li, Z.; Zhang, S.-L.; Fu, Y.; Guo, Q.-X.; Liu, L. *J. Am. Chem. Soc.* **2009**, *131*, 8815.
(11) Muto, K.; Yamaguchi, J.; Itami, K. *J. Am. Chem. Soc.* **2012**, *134*, 169.
(12) Amaike, K.; Muto, K.; Yamaguchi, J.; Itami, K. *J. Am. Chem. Soc.* **2012**, *134*, 13573.
(13) (a) Correa, A.; Cornella, J.; Martin, R. *Angew. Chem., Int. Ed.* **2013**, *52*, 1878. (b) Meng, L.-K.; Kamada, Y.; Muto, K.; Yamaguchi, J.; Itami, K. *Angew. Chem., Int. Ed.* **2013**, *52*, 10048. (c) Dermenci, A.; Dong, G. B. *Sci. China Chem.* **2013**, *56*, 685.
(14) Frisch, M. J.; Trucks, G. W.; Schlegel, H. B.; Scuseria, G. E.; Robb, M. A.; Cheeseman, J. R.; Scalmani, G.; Barone, V.; Mennucci, B.; Petersson, G. A.; Nakatsuji, H.; Caricato, M.; Li, X.; Hratchian, H. P.; Izmaylov, A. F.; Bloino, J.; Zheng, G.; Sonnenberg, J. L.; Hada, M.; Ehara, M.; Toyota, K.; Fukuda, R.; Hasegawa, J.; Ishida, M.; Nakajima, T.; Honda, Y.; Kitao, O.; Nakai, H.; Vreven, T.; Montgomery, J. A., Jr.; Peralta, J. E.; Ogliaro, F.; Bearpark, M.; Heyd, J. J.; Brothers, E.; Kudin, K. N.; Staroverov, V. N.; Kobayashi, R.; Normand, J.; Raghavachari, K.; Rendell, A.; Burant, J. C.; Iyengar, S. S.; Tomasi, J.; Cossi, M.; Rega, N.; Millam, J. M.; Klene, M.; Knox, J. E.; Cross, J. B.; Bakken, V.; Adamo, C.; Jaramillo, J.; Gomperts, R.; Stratmann, R. E.; Yazyev, O.; Austin, A. J.; Cammi, R.; Pomelli, C.; Ochterski, J. W.; Martin, R. L.; Morokuma, K.; Zakrzewski, V. G.; Voth, G. A.; Salvador, P.; Dannenberg, J. J.; Dapprich, S.; Daniels, A. D.; Farkas, O.; Foresman, J. B.; Ortiz, J. V.; Cioslowski, J.; Fox, D. J.; *Gaussian 09, revision C.01*; Gaussian Inc.: Wallingford, CT, 2010.
(15) (a) Becke, A. D. *J. Chem. Phys.* **1993**, *98*, 5648. (b) Lee, C.; Yang, W.; Parr, R. G. *Phys. Rev. B* **1988**, *37*, 785.
(16) (a) Szentpaly, L. V.; Fuentealba, P.; Preuss, H.; Stoll, H. *Chem. Phys. Lett.* **1982**, *93*, 555. (b) Dolg, M.; Wedig, U.; Stoll, H.; Preuss, H. *J. Chem. Phys.* **1987**, *86*, 866. (c) Schwerdtfeger, P.; Dolg, M.; Schwarz, W. H. E.; Bowmaker, G. A.; Boyd, P. D. W. *J. Chem. Phys.* **1989**, *91*, 1762.
(17) Hehre, W. J.; Radom, L.; Schleyer, P. v. R.; Pople, J. A. *Ab Initio Molecular Orbital Theory*; Wiley: New York, 1986.
(18) (a) Zhao, Y.; Truhlar, D. G. *Theor. Chem. Acc.* **2008**, *120*, 215. (b) Zhao, Y.; Truhlar, D. G. *Acc. Chem. Res.* **2008**, *41*, 157.
(19) Marenich, A. V.; Cramer, C. J.; Truhlar, D. G. *J. Phys. Chem. B* **2009**, *113*, 6378.
(20) Kruger, C.; Tsay, Y.-H. *J. Organomet. Chem.* **1972**, *34*, 387.
(21) (a) Verrier, C.; Martin, T.; Hoarau, C.; Marsais, F. *J. Org. Chem.* **2008**, *73*, 7383. (b) Gorelsky, S. I.; Lapointe, D.; Fagnou, K. *J. Am. Chem. Soc.* **2008**, *130*, 10848. (c) Théveau, L.; Verrier, C.; Lassalas, P.; Martin, T.; Dupas, G.; Querolle, O.; Hijfte, L. V.; Marsais, F.; Hoarau, C. *Chem.—Eur. J.* **2011**, *17*, 14450.
(22) (a) Ess, D. H.; Houk, K. N. *J. Am. Chem. Soc.* **2007**, *129*, 10646. (b) Legault, C. Y.; Garcia, Y.; Merlic, G. A.; Houk, K. N. *J. Am. Chem. Soc.* **2007**, *129*, 12664. (c) Ess, D. H.; Houk, K. N. *J. Am. Chem. Soc.* **2008**, *130*, 10187.
(23) For a review, see: van Zeist, W.-J.; Bickelhaupt, F. M. *Org. Biomol. Chem.* **2010**, *8*, 3118.
(24) (a) Fernández, I.; Bickelhaupt, F. M. *J. Comput. Chem.* **2012**, *33*, 509. (b) Gordon, C. G.; Mackey, J. L.; Jewett, J. C.; Sletten, E. M.; Houk, K. N.; Bertozzi, C. R. *J. Am. Chem. Soc.* **2012**, *134*, 9199. (c) Liang, Y.; Mackey, J. L.; Lopez, S. A.; Liu, F.; Houk, K. N. *J. Am. Chem. Soc.* **2012**, *134*, 17904. (d) Fernández, I.; Bickelhaupt, F. M.; Cossío, F. P. *Chem.—Eur. J.* **2012**, *18*, 12395. (e) Lopez, S. A.; Houk, K. N. *J. Org. Chem.* **2013**, *78*, 1778. (f) Zou, L.; Paton, R. S.; Eschenmoser, A.; Newhouse, T. R.; Baran, P. S.; Houk, K. N. *J. Org. Chem.* **2013**, *78*, 4037. (g) Fernández, I.; Sola, M.; Bickelhaupt, F. M. *Chem.—Eur. J.* **2013**, *19*, 7416. (h) Kamber, D. N.; Nazarova, L. A.; Liang, Y.; Lopez, S. A.; Patterson, D. M.; Shih, H.-W.; Houk, K. N.; Prescher, J. A. *J. Am. Chem. Soc.* **2013**, *135*, 13680. (i) Liu, F.; Paton, R. S.; Kim, S.; Liang, Y.; Houk, K. N. *J. Am. Chem. Soc.* **2013**, *135*, 15642. (j) Usharani, D.; Lacy, D. C.; Borovik, A. S.; Shaik, S. *J. Am. Chem. Soc.* **2013**, *135*, 17090. (k) Hong, X.; Liang, Y.; Griffith, A. K.; Lambert, T. H.; Houk, K. N. *Chem. Sci.* **2014**, *5*, 471. (l) Yang, Y.-F.; Cheng, G.-J.; Liu, P.; Leow, D.; Sun, T.-Y.; Chen, P.; Zhang, X.; Yu, J.-Q.; Wu, Y.-D.; Houk, K. N. *J. Am. Chem. Soc.* **2014**, *136*, 344.

(25) In the DFT study by Liu and co-workers, it was found that the C(aryl)−O activation with the $Ni(PCy_3)_2$ catalyst has an overall barrier of more than 50 kcal/mol. For details, see ref 10.

(26) We also calculated the Ni/PCy_3-catalyzed C−O activation pathways with naphthalen-2-yl benzoate, and the results are shown below. It was found that the C(aryl)−O activation for naphthalen-2-yl benzoate (**TS28-n**: 16.3 kcal/mol) is easier than that for phenyl benzoate (**TS28**: 18.2 kcal/mol, Figure 5). The C(acyl)−O activation barriers for these two benzoates are nearly identical.

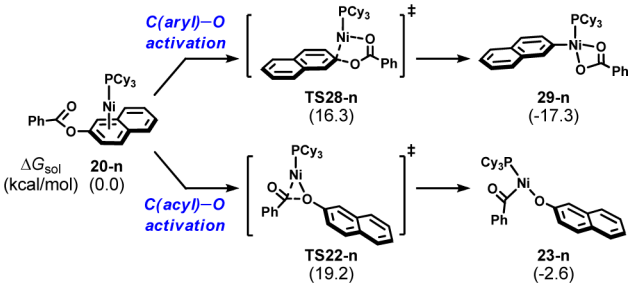

(27) The tetra-coordinated transition state **TS34-a** was also located, and it was found that **TS34-a** is 9.2 kcal/mol less favorable than the penta-coordinated transition state **TS34**.

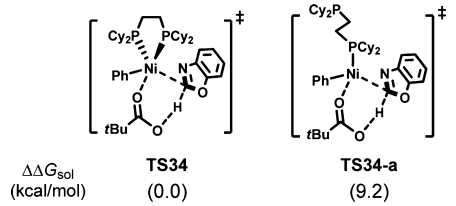

(28) Muto, K.; Yamaguchi, J.; Lei, A.; Itami, K. *J. Am. Chem. Soc.* **2013**, *135*, 16384.

(29) We also studied the reaction free energies of decarbonylation when heteroaryl groups are used, and the values (8.3 to 11.2 kcal/mol, see below) are close to that shown in Scheme 5a (R = Ph, 11.4 kcal/mol). This indicates that the choice of different aromatic substituents of acyl groups has no significant influence on decarbonylation.

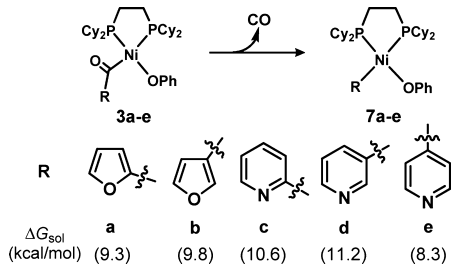

(30) (a) Bessac, F.; Alary, F.; Poteau, R.; Heully, J.-L.; Daudey, J.-P. *J. Phys. Chem. A.* **2003**, *107*, 9393. (b) Ducéré, J.-M.; Lepetit, C.; Silvi, B.; Chauvin, R. *Organometallics* **2008**, *27*, 5263. (c) Kégl, T.; Ponec, R.; Kollár, L. *J. Phys. Chem. A.* **2011**, *115*, 12463. (d) Lovitt, C. F.; Frenking, G.; Girolami, G. S. *Organometallics* **2012**, *31*, 4122.

dx.doi.org/10.1021/ja4118413 | *J. Am. Chem. Soc.* 2014, 136, 2017−2025